

TECHNICAL PHYSICS LETTERS

Founded by Ioffe Institute

Published since January 1975, 12 issues annually

Editor-in-Chief: Grigorii S. Sokolovskii

Editorial Board:

Nikita Yu. Gordeev (Deputy Editor-in-Chief), Alexey Yu. Popov (Deputy Editor-in-Chief), Grigorii S. Sokolovskii (Deputy Editor-in-Chief), Elena A. Kognovitskaya (Executive Secretary), Alexey D. Andreev, Leonid G. Askinazi, Levon V. Asryan, Nikita S. Averkiev, Nikolay A. Cherkashin, Georgiy E. Cirlin, Vladimir G. Dubrovskii, Andrey V. Dunaev, Rinat O. Esenaliev, Sergey V. Goupalov, Alexandra M. Kalashnikova, Sergey B. Leonov, Vladimir N. Mantsevich, Edik U. Rafailov, Andrei Yu. Silov, Igor V. Sokolov, Lev M. Sorokin, Valeriy V. Tuchin, Alexey B. Ustinov, Nikolay A. Vinokurov, Alexey E. Zhukov

ISSN: 1063-7850 (print), 1090-6533 (online)

TECHNICAL PHYSICS LETTERS is the English translation of ПИСЬМА В ЖУРНАЛ ТЕХНИЧЕСКОЙ ФИЗИКИ
(PIS'MA V ZHURNAL TEKHNICHESKOI FIZIKI)

Published by Ioffe Institute

15
Center-of-Mass Balanced Scanner for Scanning Probe Microscopy

© S.V. Pichakhchi, O.M. Gorbenko, S.Yu. Lukashenko, M.L. Felshtyn, I.D. Sapozhnikov, A.O. Golubok

Institute of Analytical Instrument Making, Russian Academy of Sciences, St. Petersburg, Russia
 E-mail: pichakhchi.s@yandex.ru

Received July 24, 2025
 Revised December 1, 2025
 Accepted December 1, 2025

A method for damping the low-frequency resonance of the actuator in the feedback loop of a scanning probe microscope is presented. The method is based on center-of-mass balancing of the piezoelectric actuator combined with structural symmetrization of the scanner. Numerical modeling has been used to determine the optimal scanner design. Mounting the scanner to a rigid base in the plane of geometric symmetry of the housing suppresses the low-frequency resonance, enables an increase in the open-loop gain of the feedback system, and consequently improves the response speed of the tracking system without compromising its stability. Based on the modeling results, a scanner prototype was fabricated, and its frequency response was experimentally characterized. Good agreement between the calculated and experimental data has been obtained. The advantages of low-frequency resonance damping are demonstrated by imaging a test sample surface in scanning ion conductance microscopy operated in the hopping mode.

Keywords: piezoelectric actuator, scanning speed, feedback control, center-of-mass balancing, scanning ion conductance microscopy.

DOI: 10.61011/TPL.2026.04.63190.20453

Scanning probe microscopy (SPM) is one of the basic tools of modern nanotechnology and includes scanning tunneling microscopy, various types of scanning force microscopy, near-field scanning optical microscopy, scanning ion conductance microscopy (SICM), etc. The main disadvantage of all types of SPM relative to optical and electron microscopy is the low speed of image acquisition. This is attributable to the specifics of operation of a tracking system (TS) (Fig. 1, *a*) with a negative feedback loop that stabilizes the specified interaction between a nanoprobe and the studied sample surface during precision mechanical scanning. The quality of SPM images is determined by the accuracy, speed, and stability of TS operation. It is known that the TS accuracy and speed increase with increasing open-loop gain in the feedback system, and the stability of operation of the TS is determined by its frequency response (FR) and phase-frequency characteristic [1]. The actuating element of the TS is an electromechanical scanner, which normally operates relying on the inverse piezoelectric effect [2]. Like any mechanical system, the piezo scanner has its own resonances that affect the TS speed and stability. Indeed, since the maximum useful signal frequency increases with scanning speed, the TS response speed also needs to be increased (i.e., one needs to raise unity gain frequency f_{cut} by increasing overall open-loop gain G of the feedback system). However, it is known that resonance frequency f_r of the actuating element must exceed unity gain frequency f_{cut} for the TS operation to be stable. For example, it is recommended in [3] to maintain a ratio of $f_r \approx 3f_{cut}$. Thus, on the one hand, an increase in G provides an increase in accuracy and speed of tracking; on the other hand, such an increase leads to convergence of

the values of f_{cut} and f_r (Fig. 1, *b*) and, consequently, to crossing the threshold of permissible FR gain at the resonance frequency of the scanner and narrowing of the required TS stability margin. Positive feedback in the TS and instability of SPM operation arise as a result. Therefore, one needs to damp the low-frequency resonance of the scanner or increase its frequency in order to improve performance while maintaining tracking accuracy and stability. Naturally, the resonance frequency may be increased by increasing the rigidity and reducing the size of the piezo scanner, but this will reduce its sensitivity. It was demonstrated in [4] that the low-frequency resonance of the scanner may be suppressed in a design where the position of the center of mass of a piezo actuator (PA) does not change when it is stretched and compressed. It should be noted that the so-called hopping mode [5] is usually used in SICM, where the probe is repeatedly brought closer to and shifted away from the studied sample surface. The time needed to obtain a scanning frame is increased significantly in this mode. Therefore, the task of increasing the scanning speed is especially relevant to SICM.

The aim of the present study is to increase the SICM scanning speed by damping the low-frequency resonance of the actuating element.

Figure 2, *a* shows the CAD model of the original piezo scanner design, where, just as in [4], the position of the center of mass of the PA does not change when it is compressed and stretched. Displacements were implemented by piezo actuator 5 composed of two piezo stacks $5 \times 5 \times 9$ mm in size with a central hole with a diameter of 2 mm for placing a probe in the form of a glass pipette. The elongation of one piezo stack at 120 V is $8 \mu\text{m}$. The edges of this

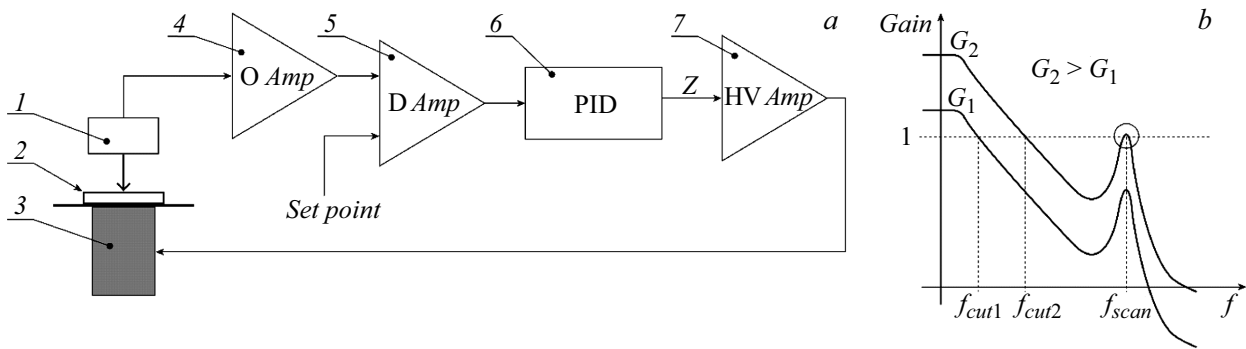


Figure 1. SPM tracking system. *a* — Block diagram: 1 — probe–sample interaction sensor, 2 — sample, 3 — Z scanner, 4 — amplifier, 5 — differential amplifier, 6 — proportional–integral–derivative controller, and 7 — high-voltage amplifier; *b* — Schematic representation of the FR of an open feedback loop at different gain factors G .

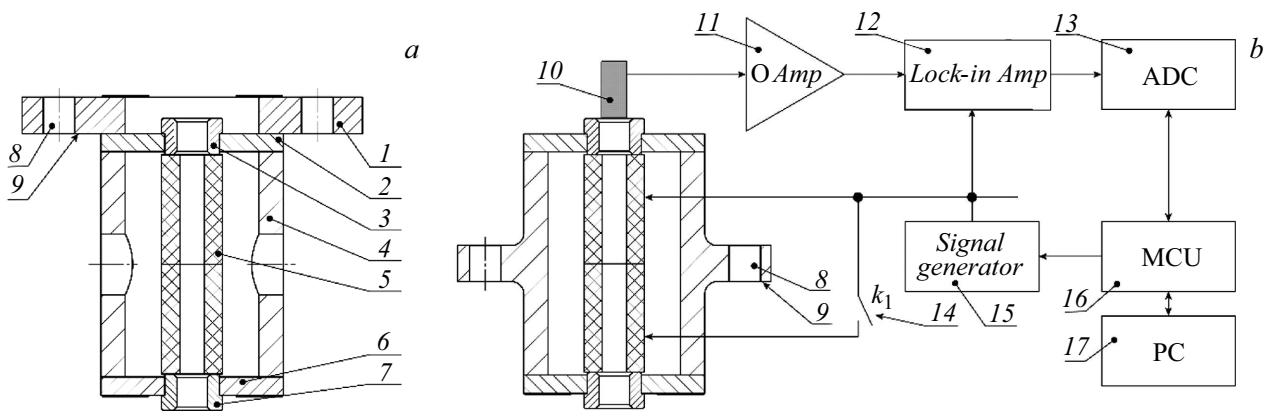


Figure 2. Scanner models with a fixed center of mass and different housing mounting options. *a* — Original design with an asymmetric housing mounting at one edge: 1 — mounting flange, 2 and 6 — membranes, 3 and 7 — bushings, 4 — scanner housing, 5 — PA composed of two piezo stacks, 8 — hole for scanner mounting, and 9 — scanner mounting plane; *b* — symmetric design with fastening along the plane of mirror symmetry of the housing and a frequency response measurement circuit: 10 — sensor, 11 — signal preamplifier, 12 — lock-in amplifier, 13 — analog-to-digital converter, 14 — switch for disabling the second piezo stack, 15 — signal generator, 16 — microcontroller, and 17 — computer.

composite PA are connected through bushings 3, 7 to elastic membranes 2, 6, which are fastened to housing 4 along the perimeter. Flange 1 serves to secure the scanner to a fixed base, which is not shown in the figure. Since piezo stacks 5 were electrically connected in parallel, the total PA elongation at 120 V was $16\ \mu\text{m}$, and the magnitude of deformation of each membrane along the scanner axis was $8\ \mu\text{m}$. The blocking force of the piezo stack was 800 N.

At the first stage, in-depth modeling of deformations and calculation of the FR of the original scanner design (Fig. 2, *a*) with rigid fastening of housing 4 to a fixed base in plane 9 with flange 1, which is located in the upper part of the housing, were performed. At the second stage, the optimal position of the mounting flange on the scanner housing providing the most effective damping of the low-frequency resonance was determined.

The piezo scanner was simulated in COMSOL using the following physical modules: solid mechanics, electrostatics with multiphysics coupling, and piezoelectric effect.

The PA was modeled as a multilayer piezo stack consisting of 82 flat parallel-connected piezoelectric elements with a thickness of 0.15 mm made of PZT-5H (lead zirconate titanate) piezoelectric ceramics. The PA was fastened to the housing at two opposite ends through elastic metal membranes. The thickness of these membranes was chosen so that the calculated elastic force arising during their deformation did not exceed the blocking force of the piezo stack. As in [6], the relation between the polarization of the material and its deformation in the stress–charge form was chosen for a complete description of the piezoelectric effect:

$$T_{i,j} = \sum_{k,l} c_{Eijkl} S_{kl} + \sum_k e_{ijk}^t E_k, \quad (1)$$

$$D_i = \sum_{j,k} e_{ijk} S_{jk} + \epsilon_0 \sum_j \epsilon_{rSij} E_j. \quad (2)$$

Here, \mathbf{T} is the mechanical stress tensor, \mathbf{S} is the strain tensor, \mathbf{E} is the electric field strength vector, \mathbf{D} is the polarization vector, c_E is the material rigidity, e are the parameters of

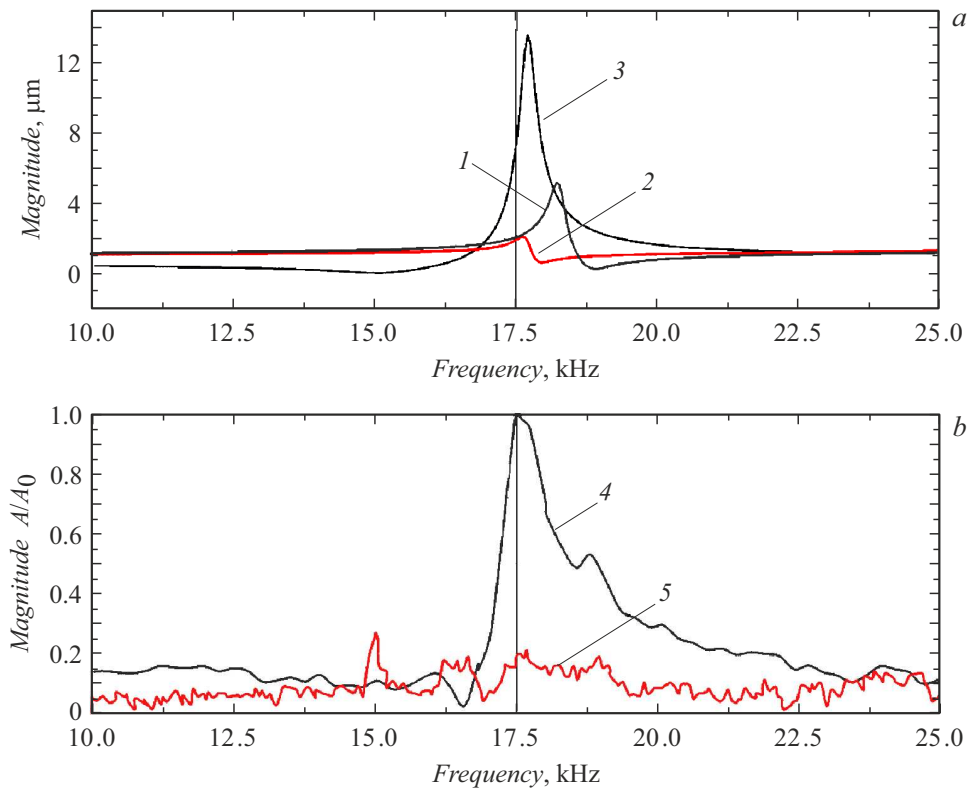


Figure 3. Scanner FR. *a* — Calculation results: 1 — balanced design with a fixed center of mass and asymmetric housing mounting, 2 — balanced design with symmetric housing mounting in the plane of mirror symmetry, and 3 — unbalanced design with symmetric housing mounting; *b* — experimental data: 4 — unbalanced design and symmetric housing mounting and 5 — balanced design and symmetric housing mounting.

interrelation, $\epsilon_{r,S}$ is the relative permittivity at constant strain, and ϵ_0 is the permittivity of vacuum. Quantities c_E , e , and $\epsilon_{r,S}$ are tensors of the fourth, third, and second rank, respectively, and may be presented as matrices.

The numerical value of element e_{33} in the matrix of interrelations e (elasticity matrix), which determines the magnitude of deformations in the direction of polarization of the piezoelectric material, was chosen so that the sensitivities of modeled and actual PAs were the same (a $16\ \mu\text{m}$ elongation at a voltage of 120 V).

The scanner design shown in Fig. 2, *a* was imported into the COMSOL model directly from the CAD file. The parameters of structural steel were used for calculation of all structures except the PA.

Boundary conditions were set so as to correspond to the method of scanner mounting in an actual experiment. The hinge boundary condition was assigned to bolt holes 8, and the roller boundary condition was set on scanner mounting plane 9. Since the rigidity of the flange is much greater than the rigidity of the membranes and it is fixed to a massive base, its deformation in the process of operation may be neglected. On these grounds, the contact of heads of fastening screws with the flange and the contact of the flange with the base are also neglected in the model.

The calculation revealed that the housing of the original scanner model with asymmetric fastening to the base

(Fig. 2, *a*) undergoes a noticeable deformation in the process of oscillations, and the corresponding FR curve (1 in Fig. 3, *a*) features a pronounced low-frequency resonance.

We attribute the observed poor resonance damping in the original scanner design to the deformation of housing 4 and, as a consequence, to the difference in compression forces acting on piezo actuator 5 from above and below, which shift the position of the center of mass.

To equalize the forces acting on the PA, mounting flange 1 was shifted to the geometric center of the housing so that the plane of contact of the flange with the fixed base divided the housing into two parts of equal rigidity. As a result, the elastic influences of the housing exerted on the PA from above and below were compensated (Fig. 2, *b*).

This shift of the housing mounting plane suppressed the peak in the scanner FR (curve 2 in Fig. 3, *a*). To compare the designs with stationary and moving positions of the PA center of mass, we plotted (see the same figure) the FR calculated for identical symmetrical fastening of the housing, but with voltage applied to one half of the PA only. It can be seen that the low-frequency FR peak (curve 3 in Fig. 3, *a*) in this case is several times higher than the peak corresponding to the stationary position of the PA center of mass.

Based on the modeling data, a prototype of an optimal scanner with a mounting flange at the center of its

housing was designed and fabricated. Figure 2, *b* shows the FR measurement diagram. Compact piezo stack $10 \times 2 \times 5$ mm in size was used as a vibration sensor in measurements of the piezo scanner FR. One edge of this piezo stack/sensor was fixed to bushing 3, and the other one remained free. To measure the FR, the voltage generator signal was applied to the PA and drove the scanner at frequency f . Voltage was applied to both piezo stacks and just one of them in experiments for the scanner design with a fixed center of mass and the unbalanced design, respectively. Signals from the sensor and a signal generator were fed to the input and the reference input of a lock-in amplifier, respectively. The signal at the lock-in amplifier output was proportional to the amplitude of piezo scanner oscillations at frequency f .

Figure 3, *b* shows the experimentally measured FRs of the scanner with symmetrical housing fastening and two types of piezo stack connection corresponding to fixed and moving positions of the center of mass. It is evident (curve 5 in Fig. 3, *b*) that the balanced connection of piezo stacks (with voltage applied to both of them) induces considerable suppression of the low-frequency resonance. One can also see that the calculated (curve 3 in Fig. 3, *a*) and experimentally measured (curve 4 in Fig. 3, *b*) FRs for the design with a moving center of mass (with voltage applied to one half of the PA in calculations and to one of the two piezo stacks in experiments) agree closely. The difference between the calculated and experimentally measured resonance frequencies is less than 1%.

The examined scanner was tested in optimized (Fig. 2, *b*) and original (Fig. 2, *a*) designs as a Z-scanner in a „home-made“ SICM system. The frame acquisition time in the hopping mode was measured by scanning a test sample in the form of a polymer cast taken from a TGX1 periodic silicon lattice. Scanning was performed at the maximum open-loop gain: the slightest increase in gain destabilized the TS operation. Experiments with different sample types revealed a four-fold reduction in image acquisition time when the optimized balanced scanner was used.

Figure 4 shows an example SICM image obtained using the optimally balanced scanner.

Thus, a COMSOL model of a scanner for SPM with a fixed position of the center of mass was constructed. The adequacy of this model was verified by a close agreement between the calculated and experimentally measured scanner FRs. Calculations performed using the developed model provided an opportunity to design a scanner that is optimal in terms of low-frequency resonance damping efficiency. It was demonstrated that one needs to choose the optimal mounting of the scanner to a fixed base, ensuring the equality and counter-directionality of forces acting on the PA and ultimately stabilizing the position of the center of mass.

The scanner was tested as part of a „home-made“ SICM system in the hopping mode. These tests revealed that the proposed approach with damping of the low-frequency resonance of the SPM scanner allows for a significant

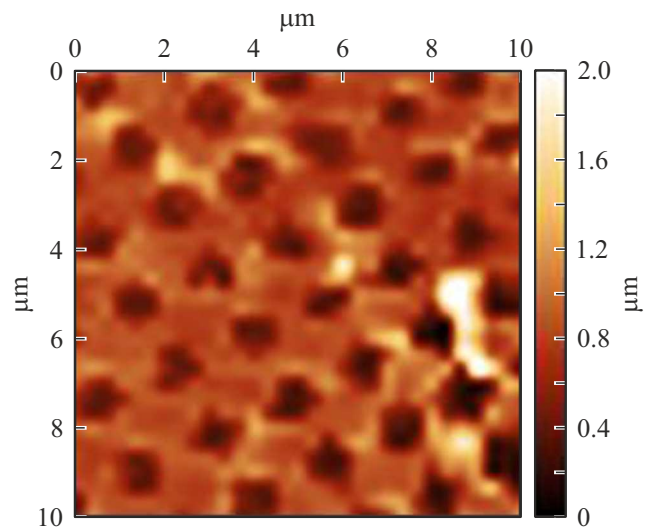


Figure 4. SICM image of the surface of a test sample in the form of a polymer cast from a TGX1 Si lattice. The image was obtained in the hopping mode by the optimally balanced scanner.

increase in scanning speed, which is especially important for hopping-mode operation with the probe being repeatedly brought closer to and shifted away from the sample surface.

Funding

This study was supported by the Ministry of Education and Science of the Russian Federation (project No. 075-00444-25-00).

Conflict of interest

The authors declare that they have no conflict of interest.

References

- [1] E.I. Yurevich, *Teoriya avtomaticheskogo upravleniya*, 3rd ed. (BKhV-Peterburg, SPb., 2007), pp. 122–126 (in Russian).
- [2] N. Kodera, H. Yamashita, T. Ando, *Rev. Sci. Instrum.*, **76** (5), 053708 (2005). DOI: 10.1063/1.1903123
- [3] D.W. Pohl, *IBM J. Res. Dev.*, **30** (4), 417 (1986). DOI: 10.1147/rd.304.0417
- [4] S. Watanabe, S. Kitazawa, L. Sun, N. Kodera, T. Ando, *Rev. Sci. Instrum.*, **90** (12), 123704 (2019). DOI: 10.1063/1.5118360
- [5] S.V. Pichahchi, O.M. Gorbenko, S.Yu. Lukashenko, M.L. Felshtyn, I.D. Sapozhnikov, I.S. Svaikin, A.O. Golubok, *Tech. Phys. Lett.*, **50** (10), 95 (2024). DOI: 10.61011/TPL.2024.10.59707.19984
- [6] O.M. Gorbenko, S.Y. Lukashenko, S.V. Pichahchi, I.D. Sapozhnikov, M.L. Felshtyn, A.O. Golubok, *Nanosyst.: Phys., Chem., Math.*, **15** (5), 643 (2024). DOI: 10.17586/2220-8054-2024-15-5-643-653

Translated by D.Safin